0026-895X/09/7602-440–450$20.00
MOLECULAR PHARMACOLOGY
Vol. 76, No. 2
54650/3500013
Mol Pharmacol 76:440–450, 2009
Printed in U.S.A.

Docking of 1,4-Benzodiazepines in the α_1/γ_2 $GABA_A$ Receptor Modulator Site[S]

D. Berezhnoy, T. T. Gibbs, and D. H. Farb

Laboratory of Molecular Neurobiology, Department of Pharmacology & Experimental Therapeutics, Boston University School of Medicine, Boston, Massachusetts

Received January 8, 2009; accepted May 29, 2009

ABSTRACT

Positive allosteric modulation of the $GABA_A$ receptor ($GABA_AR$) via the benzodiazepine recognition site is the mechanism whereby diverse chemical classes of therapeutic agents act to reduce anxiety, induce and maintain sleep, reduce seizures, and induce conscious sedation. The binding of such therapeutic agents to this allosteric modulatory site increases the affinity of GABA for the agonist recognition site. A major unanswered question, however, relates to how positive allosteric modulators dock in the 1,4-benzodiazepine (BZD) recognition site. In the present study, the X-ray structure of an acetylcholine binding protein from the snail *Lymnea stagnalis* and the results from site-directed affinity-labeling studies were used as the basis for modeling of the BZD binding pocket at the α_1/γ_2 subunit interface. A tethered BZD was introduced into the binding pocket, and molecular simulations were carried out to yield a set of candidate orientations of the BZD ligand in the binding pocket. Candidate orientations were refined based on known structure-activity and stereospecificity characteristics of BZDs and the impact of the α_1H101R mutation. Results favor a model in which the BZD molecule is oriented such that the C5-phenyl substituent extends approximately parallel to the plane of the membrane rather than parallel to the ion channel. Application of this computational modeling strategy, which integrates site-directed affinity labeling with structure-activity knowledge to create a molecular model of the docking of active ligands in the binding pocket, may provide a basis for the design of more selective $GABA_AR$ modulators with enhanced therapeutic potential.

$GABA_A$ receptors ($GABA_ARs$) are pentameric transmembrane proteins that belong to the cysteine-loop superfamily of ligand-gated ion channels and function as GABA-gated Cl^--selective channels, which mediate most fast inhibitory neurotransmission in the central nervous system (Berezhnoy et al., 2007). There are 20 related $GABA_AR$ subunits in mammals, designated α_{1-6}, β_{1-4}, γ_{1-3}, δ, ε, π, θ, and ρ_{1-3}, that can assemble in multiple combinations to produce different $GABA_AR$ subtypes (Barnard et al., 1998; Bonnert et al., 1999). The regional and cellular distribution of different $GABA_AR$ subunits is distinct but overlapping, and individual receptor subtypes exhibit distinct subcellular localizations (Berezhnoy et al., 2007). Most $GABA_ARs$ in the adult mammalian central nervous system are composed of α, β, and γ subunits, with $\alpha_1\beta_{2/3}\gamma_2$ being the most abundant subtype (Sieghart and Sperk, 2002).

$GABA_ARs$ are activated by binding of agonist to recognition sites located at $\alpha(-)/\beta(+)$ subunit interfaces (Berezhnoy et al., 2007). Agonist-induced receptor activation can be modulated through allosteric binding sites located at the $\alpha_1(+)/\gamma_2(-)$ subunit interface (the BZD recognition site) (Choh et al., 1977; Chan and Farb, 1985). Residues implicated in the formation of the GABA and BZD binding sites are located at equivalent positions within six loops in the extracellular N-termini of the α, β, and γ subunits (Supplemental Fig. 1) (Berezhnoy et al., 2007).

Previous attempts have been made to superimpose the structures of allosteric modulators to construct a pharmacophore model for the BZD recognition site (Borea et al., 1987; Villar et al., 1989; Schove et al., 1994; Zhang et al., 1995; Huang et al., 1998, 1999; He et al., 2000; Marder et al., 2001; Verli et al., 2002). However, such models are difficult to relate to receptor structure. Sigel et al. (1998) determined affinities for a series of imidazo- and 5-phenyl-1,4-benzodiaz-

This work was supported by the National Institutes of Health National Institute of Mental Health [Grant R01-MH049469].

Article, publication date, and citation information can be found at http://molpharm.aspetjournals.org.

doi:10.1124/mol.109.054650.

[S] The online version of this article (available at http://molpharm.aspetjournals.org) contains supplemental material.

ABBREVIATIONS: $GABA_AR$, $GABA_A$ receptor; BZD, benzodiazepine; FNZ, flunitrazepam; DZ, diazepam; RMSD, root-mean-square deviation; DZ-NCS, diazepam carrying a thiol-reactive –N=C=S group; AChBP, acetylcholine binding protein; Ro 15-4513, 4H-imidazo(1,5-*a*)(1,4)benzodiazepine-3-carboxylic acid, 8-azido-5,6-dihydro-5-methyl-6-oxo-, ethyl ester; Ro 15-1788, 8-fluoro-5,6-dihydro-5-methyl-6-oxo-4*H*-imidazo[1,5-*a*][1,4]benzodiazepine-3-carboxylic acid ethyl ester.

epines to wild-type and mutant receptors to delineate the orientation of these ligands in the recognition site. An extra hydroxyl group of tyrosine introduced by the γ_2F77Y mutation interferes with para-substitutions of the C5-phenyl ring, suggesting that the phenyl ring is adjacent to γ_2Phe77 in the binding pocket (Sigel et al., 1998). Kucken and colleagues (2003) used a series of three substituted imidazobenzodiazepines in combination with amino acid mutations of varying volume at γ_2Ala79 to infer the position of compounds similar to Ro 15-1788 and Ro 15-4513 (Kucken et al., 2003). Photoaffinity labeling using [^{3}H]flunitrazepam identified the major site that incorporates radioactivity as His101 of loop A (McKernan et al., 1995; Davies et al., 1996; Duncalfe et al., 1996) and a second less abundant site as Pro96 (Smith and Olsen, 2000). Likewise, photoaffinity labeling using the imidazobenzodiazepine [^{3}H]Ro 15-4513 identified residue Tyr209 of loop C of the α_1 subunit as proximal to the benzodiazepine binding site (Sawyer et al., 2002). However, the docking position with respect to specific contact residues cannot be deduced because of uncertainty of photoaffinity labeling in an environment containing multiple aromatic residues (Kotzyba-Hibert et al., 1995). Using a C7-modified diazepam (DZ) carrying a thiol-reactive –N=C=S group (DZ-NCS), α_1H101C was confirmed to be in or near the binding pocket. At the functional level, the reacted receptor becomes irreversibly locked in a positively modulated state (Berezhnoy et al., 2004, 2005; Tan et al., 2007a,b,c).

To further refine the positioning of ligands in the BZD binding pocket, we use a homology model based on the crystal structure of AChBP (Brejc et al., 2001). The initial ligand position was obtained by modeling DZ-NCS covalently linked to α_1H101C (Fig. 1). This yields two candidate orientations, one with the C5-phenyl group oriented approximately parallel to the cell membrane, and the other with the C5-phenyl oriented parallel to the ion channel. We evaluated the consistency of these orientations with respect to four criteria: 1) the capacity to accommodate a tethered DZ analog ([poly(MeBZD)] that was used in the early affinity column purification of $GABA_A$ receptors (Sigel et al., 1983; Sigel and Barnard, 1984); 2) the effect of the α_1H101R mutation, which abolishes BZD binding (Wieland et al., 1992; Wieland and Lüddens, 1994; Benson et al., 1998; Dunn et al., 1999); 3) the two enantiomers of 3-methyl-substituted FNZ, Ro 11-6896 and Ro 11-6893 (Niehoff et al., 1982; De Blas et al., 1985); and 4) the binding affinities of a set of active and inactive BZD derivatives (Klopman and Contreras, 1985; Zhang et al., 1994) (Fig. 2). The results show that the docking orientation with the C5-phenyl parallel to the membrane satisfies all of these criteria, whereas the orientation with the phenyl parallel to the ion channel does not, indicating that the former orientation in the binding pocket is favored.

Materials and Methods

Homology Modeling. A homology model of the extracellular domain of the rat $GABA_AR$ α_1 and γ_2 subunits was constructed based on the X-ray structure of the AChBP complexed with nicotine (Protein Data Bank entry 1uw6) (Celie et al., 2004). The mature protein sequences of the rat α_1 and γ_2 subunits (accession numbers: α_1, P62813; γ_2, P18508) were aligned with sequences of two adjacent AChBP subunits (A and B, respectively) using ClustalW (Thompson et al., 1994) (Supplemental Fig. 1). Because the $GABA_AR$ subunits share only ~18% identity with AChBP, the reliability of the alignment was checked by creating a multiple alignment with all α_{1-6} and γ_{1-3} subunits and α, β, γ, and δ subunits of the nicotinic acetylcholine receptor, taking the secondary structure predictions into account. Using absolutely conserved residues to "anchor" regions of low homology, we edited the sequence alignment to align gaps with loops in the AChBP structure.

Three regions of the $GABA_A$ receptor subunits did not align well: the N-terminal α-helix, the region between β-sheet domains β4 and β6, and the region between β-sheet domains β8 and β9 (Supplemental Fig. 1). In contrast to the alignment of Brejc et al. (2001), we have aligned the insertion between β-sheet domains β4 and β6 of the $GABA_A$ receptor with the β4–β5 extracellular loop of AChBP. This results in a better alignment with the $GABA_AR$ subunits, because there is more room for the inserted residues compared with the Brejc et al. alignment, in which the β5–β6 β-sheet domain is partially buried. After alignment, each subunit was modeled independently using the Build Homology Model module of Discover Studio (Accelrys, San Diego, CA). Loops to fill in the gaps between the $GABA_ARs$ sequences and the template sequence were built and refined using the autorotomer feature of the same module. The backbone atoms of each residue were tethered to the coordinates of corresponding residues in the AChBP template with a force constant of 5 kcal · $Å^{-1}$. This protocol generated 10 receptor dimer models, which were then subjected to energy minimization to eliminate obvious problems such as steric clashes, and the model with the lowest occurrence of unfavorable contacts was chosen.

In the resulting dimer model, ~98% of the residues have a backbone geometry falling in favorable regions of the Ramachandran plot. Superimposing the ligand binding domain of the homology model onto the AChBP yields an average root-mean-square deviation of 0.7 Å for α-carbons. When the consensus sites for *N*-glycosylation are mapped onto the model, all are found on the solvent-accessible surface. Residues previously identified as forming the GABA and BZD binding sites are also on the water-accessible surface, with the exception of γ_2Met57. The available evidence indicates that our homology model is based on the structure of the AChBP in a conformational state that binds nicotine with high affinity and is thus presumed to resemble a conformation of the nAChR that binds ACh with high affinity (i.e., either an open or desensitized state) (Brejc et al., 2001; Unwin et al., 2002; Unwin, 2003; Celie et al., 2004). A number of the residues that this alignment predicts to line the BZD binding pocket, to our knowledge, have not been investigated experimentally. In particular, Lys155, Thr213, and His215 on the α_1 subunit and Asn60 on the γ_2 subunit are predicted to face the interior of the binding pocket and are located in close proximity to residues shown to affect potency of efficacy of BZD site ligands.

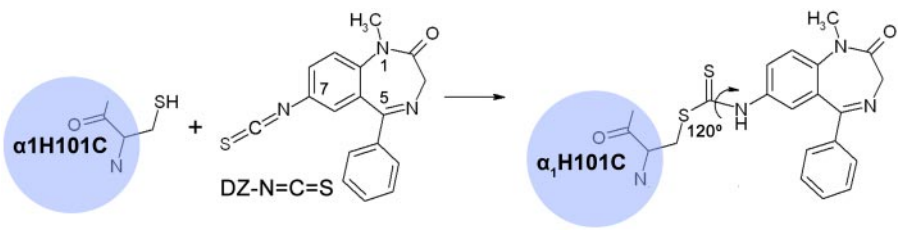

Fig. 1. Mechanism of covalent modification by DZ-NCS: nucleophilic attack of α_1H101C on DZ-NCS results in an α_1 substituent bearing DZ covalently linked to the drug recognition site. In the resulting product, the angle formed by –C–S–C– bond is 120° and allows some degree of rotation around the –C–S–, –S–C–, and –C–N– bonds.

Modeling of DZ-NCS Tethered to $\alpha_1\gamma_2$ BZD Binding Pocket. After optimization of the receptor model, the α_1H101C mutation was introduced, covalently linked to DZ-NCS corresponding to the covalent reaction of cysteine with the -NCS reactive group. 1,4-Benzodiazepines such as DZ exist in solution as an equimolar mixture of two chiral conformers due to rapid inversion of the nonplanar seven-membered ring (Blount et al., 1983). Both conformers of DZ-NCS were therefore used for docking studies, rather than the single conformation of DZ found in the X-ray structure (Camerman and Camerman, 1972) (Fig. 3). During simulation, constraints were applied to the receptor model such that only the ligand and the residues facing the interior of the binding pocket were allowed to move: on the α_1 subunit: Phe99, His101, Asn102, Lys155, Tyr159, Thr162, Gly200, Val202, Ser204, Ser205 Thr206, Val211, Thr213, and His215; on the γ_2 subunit: Asp56, Tyr58, Asn60, Asp75, Phe77, Ala79, Thr81, Thr126, Met130, Leu140, Thr142, Arg144, Lys184, Ser186, Val188, Val190, Thr193, Arg193, and Trp196.

Conformations were searched by rotation of the -CS-NH- bond in 30° increments, followed by a standard dynamics cascade procedure that included minimization steps, simulated annealing (600 to 50 K), equilibration, and production steps at 300 K. This resulted in a pool of DZ-NCS conformations. Ligand orientations in which the C5-phenyl extended out of the recognition site were discarded, because the C5-phenyl is essential for high-affinity binding of 1,4-BZDs (Sigel et al., 1998), and ligands that do not have this moiety are inactive (i.e., Ro 5-4654; Fig. 2A), indicating that the phenyl group is likely to be an interaction center.

This procedure yielded two favorable orientations, designated "h" (horizontal) and "v" (vertical), for each of the two conformers of DZ-NCS, for a total of four candidate models of bound DZ-NCS, designated DZ-NCS1h, DZ-NCS1v, DZ-NCS2h, and DZ-NCS2v (Fig. 5). Corresponding models for DZ and FNZ bound to the receptor were obtained as follows for each of the candidate models: the bond between the DZ-NCS molecule and the receptor was eliminated; the native histidine-101 residue of the receptor was restored; and DZ-NCS was replaced by DZ, FNZ, or other BZD derivatives (Fig. 2). Subsequently, each model was subjected to the standard dynamics cascade protocol as described above. Interaction energies were calculated using Calculate Interaction Energy: ligand and receptor were defined as groups of atoms, dielectric constant was set to 1, nonbound list radius was 14, and nonbound higher and lower cutoff distances were set to 12 and 10, respectively.

Automated Ligand Docking. Docking of DZ and FNZ was carried out using the CDOCKER algorithm (Wu et al., 2003) in the

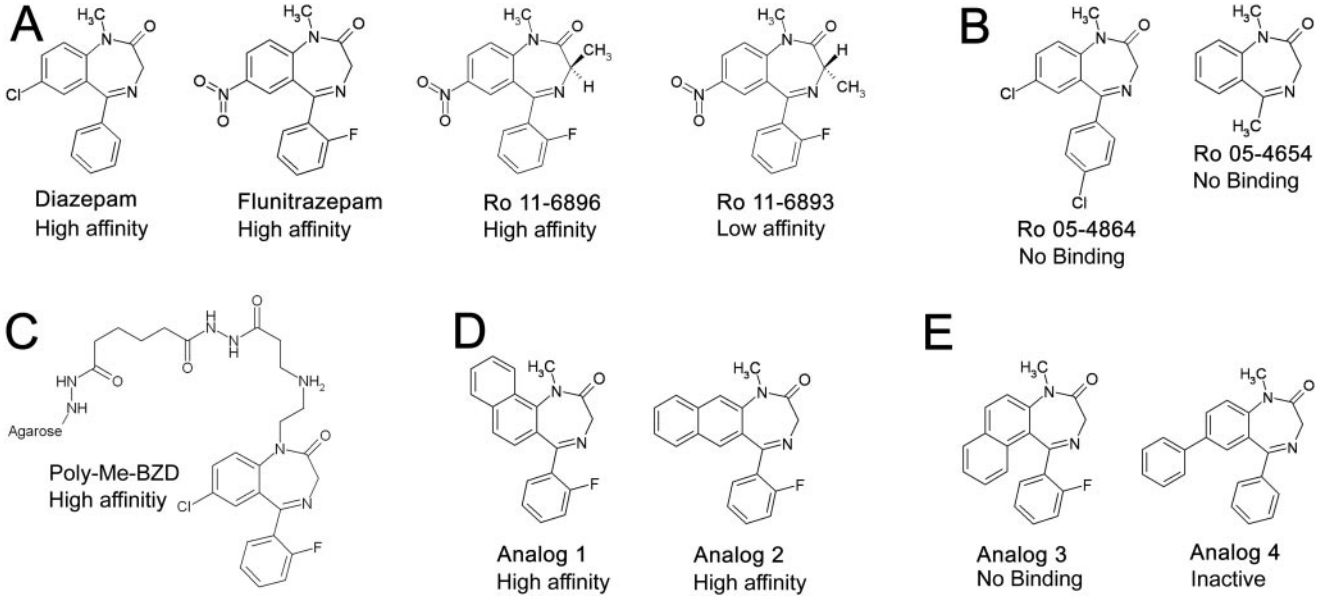

Fig. 2. Structures of BZD derivatives used in docking studies. A, BZD modulators diazepam, flunitrazepam, and flunitrazepam derivatives Ro 11-6896 and Ro 11-6893 carrying an optically active methyl group at the 3-position. B, inactive compounds Ro 05-4864 and Ro 05-4654 do not bind. C, structure of BZD ligand used by Sigel et al. (1983) to isolate the $GABA_AR$. D and E, structures of active (D) and inactive (E) BZD analogs used to test model of ligand orientation. High-affinity indicates ligands with IC_{50} <100 nM; low affinity indicates ligands with 100 nM < IC_{50} < 1 μM. Compounds identified as inactive have IC_{50} > 1 μM (Ro 05-4864, Ro 05-4854, analog 3) or lack activity in behavioral assays (analog 4).

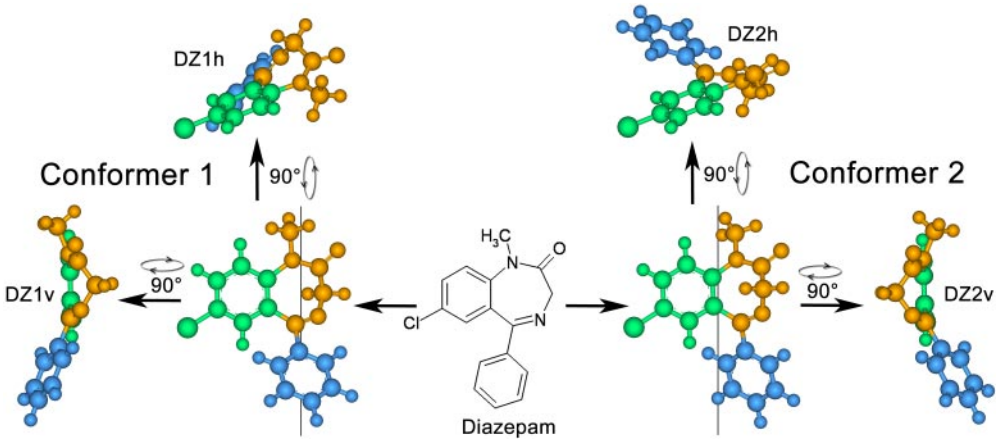

Fig. 3. Diazepam exists in solution as equimolar mixture of conformers, denoted as DZ1 and DZ2, defined as shown. Simulations identified two candidate orientations for DZ in the binding pocket. Each conformer can potentially bind in either an h- or v-orientation. These are denoted DZ1h and DZ1v for conformer DZ1 and DZ2h and DZ2v for conformer DZ2.

Discovery Studio environment. CDOCKER is a grid-based molecular docking method that uses the CHARMm force field. The receptor is held rigid while the ligand is allowed to flex during the refinement process. The binding site cavity for automated docking was assigned via the protein-ligand interaction menu with a sphere of 8 Å. A set of 20 random ligand conformers was generated from the initial ligand structure through high-temperature molecular dynamics followed by random rotations and then refined by grid-based (GRID I)-simulated annealing and energy minimization. The simulated annealing procedure consisted of 1000 steps of variable temperature molecular dynamics. In each cycle, the temperature was scaled from 600 to 50 K over an interval of 10 ps followed by Smart Minimizer energy minimization to 0.1 kcal $\cdot$ mol^{-1} $\cdot$ Å^{-1}. The 20 most energy-favorable ligand conformers were selected for further analysis. Both FNZ and DZ converged on a set of similar conformations for both manual and automated docking procedures, consistent with a restricted stereospecific binding site.

Results

Modeling of the $\alpha_1\gamma_2$ BZD Binding Pocket. One of the main challenges of homology modeling is to identify the correct sequence alignment. The ligand-binding domains of the GABA$_A$R subunits share only ~18% amino acid identity with AChBP, which is marginal for effective alignment and homology modeling. The validity of the GABA$_A$R model is supported by its consistency with available biochemical data on the location of critical residues (i.e., glycosylation sites, residues forming GABA, and BZD binding sites). Residues residing at the α_1 subunit that have been reported to contribute to the BZD binding pocket (His101, Tyr159, Thr162, Gly200, Ser204, Ser205, Thr206, Tyr209, and Val211) are all water-exposed, as were all such residues on the γ_2 subunit (Tyr58, Asp75, Phe77, Ala79, Thr81, Met130, Leu140, Thr142, Arg144, Lys184, Ser186, Val188, Val190, Thr193, Arg194, and Trp196), with the single exception of γ_2Met57 (Fig. 4).

Modeling of DZ-NCS Linked to the BZD Binding Site. To determine how BZDs fit into the binding site, the assumption was made that all active BZD-like ligands orient themselves similarly in the binding pocket. An important constraint is provided by the observation that DZ-NCS retains modulatory activity when covalently linked to a cysteine introduced by mutagenesis in place of histidine at position $\alpha_1$101, a locus that has been identified by mutational analysis as critical for BZD binding. We simulated the covalent linkage of a DZ-NCS molecule (Fig. 2) in two alternative conformations to the α_1H101C mutated receptor, because it has been shown that 1,4-benzodiazepines in solution exist as mixture of two conformers that have an inversion barrier of ~12 kcal/mol (Fig. 3) (Blount et al., 1983). Modeling indicates that each conformer can potentially assume two favorable orientations when bound to α_1H101C: a horizontal (h) orientation in which the phenyl group is approximately parallel to the plane of the plasma membrane, and a vertical (v) orientation in which the phenyl group extends toward the membrane, approximately parallel to the axis of the ion channel (Fig. 5).

In the h orientation, the benzodiazepine ring lies in the

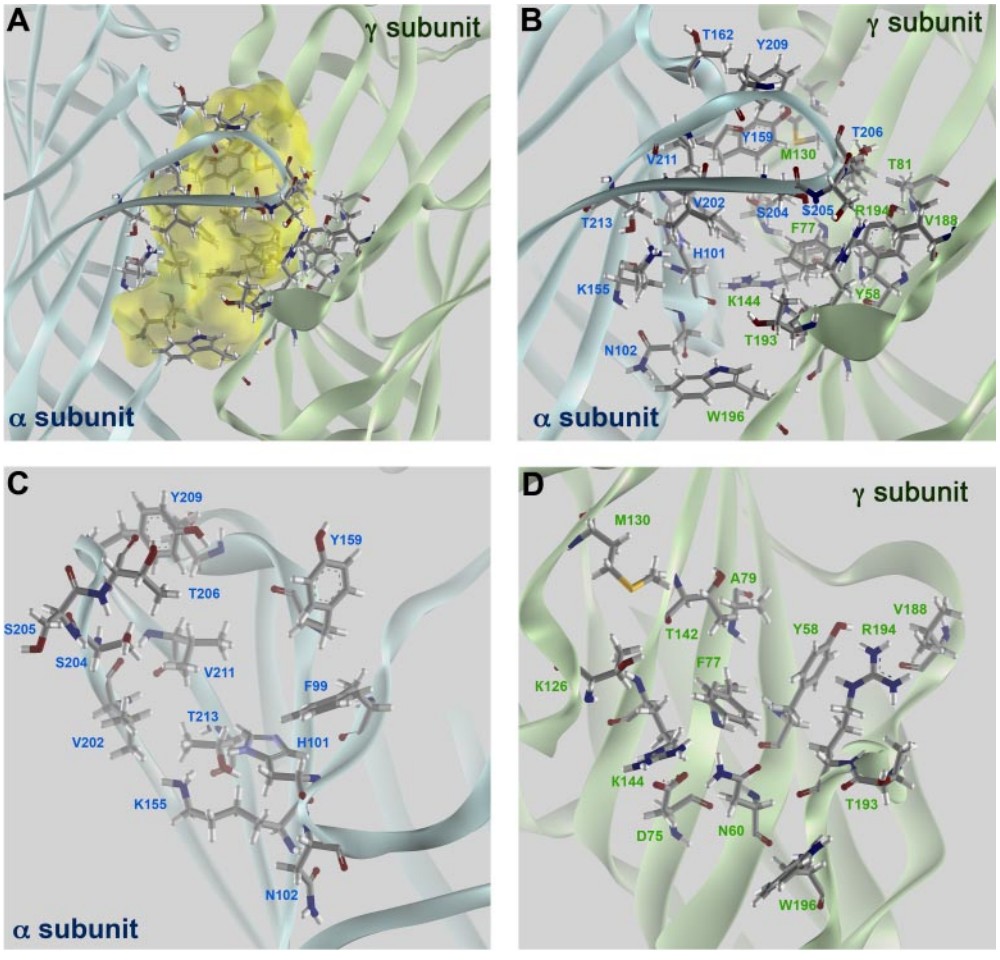

Fig. 4. Structure of BZD binding pocket. The BZD binding site of $\alpha\beta\gamma$ GABA$_A$Rs is formed at the $\alpha(+)/\gamma(-)$ subunit interface. A, mapping of accessible volume of the BZD binding pocket. B, front view of the binding pocket. Residues on the α subunit facing the interior of the binding site are labeled in black, and those on the γ subunit are labeled in blue. C and D, views of the α and γ subunits from inside the BZD binding pocket. Residues that are believed to affect properties of BZD ligands via direct contact or through indirect/allosteric effects are identified.

same plane as α_1Phe99 and γ_2Phe77, the C5-phenyl group is directed toward α_1Tyr159, and the carboxyl groups are directed toward α_1Ser204 and γ_2Arg194 (Fig. 5, A and B). The main difference between conformers 1 and 2 is the orientation of the N1 methyl group: in conformer 1 (DZ-NCS-1h), it is directed toward γ_2Thr193, whereas in conformer 2 (DZ-NCS-2h), the N1 methyl group is directed out of the binding pocket (Figs. 5C and 8D).

In the v-orientation, the C5-phenyl group is oriented parallel to the intersubunit interface and lies in close proximity of γ_2Trp196 (Fig. 5, E and G). In conformer 1 (DZ-NCS-1v), N1 methyl group is directed out of the binding pocket (Fig. 5F), whereas in conformer 2 (DZ-NCS-2h), it is directed toward the interior of the binding pocket (Fig. 5H).

Because irreversible binding of DZ-NCS results in persistent $GABA_A$ receptor potentiation, it is likely that the orientation of covalently bound DZ-NCS corresponds to the orientation of other active benzodiazepine site ligands in the binding pocket. These four orientations were thus used as a basis for modeling the binding of DZ and FNZ. All models were subsequently subjected to energy minimization.

Modeling of DZ and FNZ Binding. The classic 1,4-BZDs DZ and FNZ were then introduced the same position. Energy minimization runs resulted in orientations that were close to the original position. The only minor difference between the two was caused by the presence of a fluorine atom, resulting in a slight rotation of the C5 phenyl of FNZ molecule. It is noteworthy that this rotation brings the fluorine atom closer to hydroxyl group of α_1Tyr209. For both DZ (Fig. 6) and FNZ (Fig. 7), the C7-substituent of both ligands is located in close proximity to α_1His101 and α_1Lys155, and this is especially pronounced with FNZ, which has a strongly electronegative nitro group that can participate in the hydrogen bonding with both α_1His101 and α_1Lys155. The carbonyl group of both ligands faces the α_1Ser204-γ_2Thr193-γ_2Arg194 triad, where it can form hydrogen bonds and coordinate two domains: the tip of loop C, and most of loop F. As with DZ-NCS, DZ and FNZ can exist in two conformers, which may be positioned in either the h- or v-orientation. The orientation of the C5-phenyl is a major difference between h- and v-orientations for both DZ and FNZ. With ligand in the h-orientation, the C5-phenyl is located in the same plane as α_1Phe99 and γ_2Phe77. These residues together form a "floor" to the binding pocket. The "ceiling" of the binding pocket is formed by α_1Thr206 and α_1Tyr209 (Figs. 6 and 7).

Replacement of α_1His101 with arginine abolishes the binding of classic 1,4-benzodiazepines, so we examined the impact of this mutation on the interaction of DZ and FNZ with the binding pocket. In the h-orientation, severe steric interference is evident for both conformers of DZ and FNZ between the arginine residue and the aromatic moiety adjacent to the benzodiazepine ring and the C5-phenyl group, resulting in considerably unfavorable energies of interaction (Table 1). In the v-orientation, binding of DZ and FNZ is somewhat destabilized but remains energetically favorable, with the benzodiazepine ring and nitro group fitting between the α_1H101R and α_1Lys155 residues (Fig. 6 and 7). The profound impact of the α1H101R mutation on binding is thus more consistent with DZ and FNZ being bound in the h-orientation.

The γ_2F77Y mutation has been shown to decrease binding affinities of both DZ and FNZ by ~226- and ~170-fold in radioligand binding experiments but does not affect DZ potency in electrophysiological experiments (Buhr et al., 1997). As modeled, the γ_2F77Y residue faces the BZD ligands in the

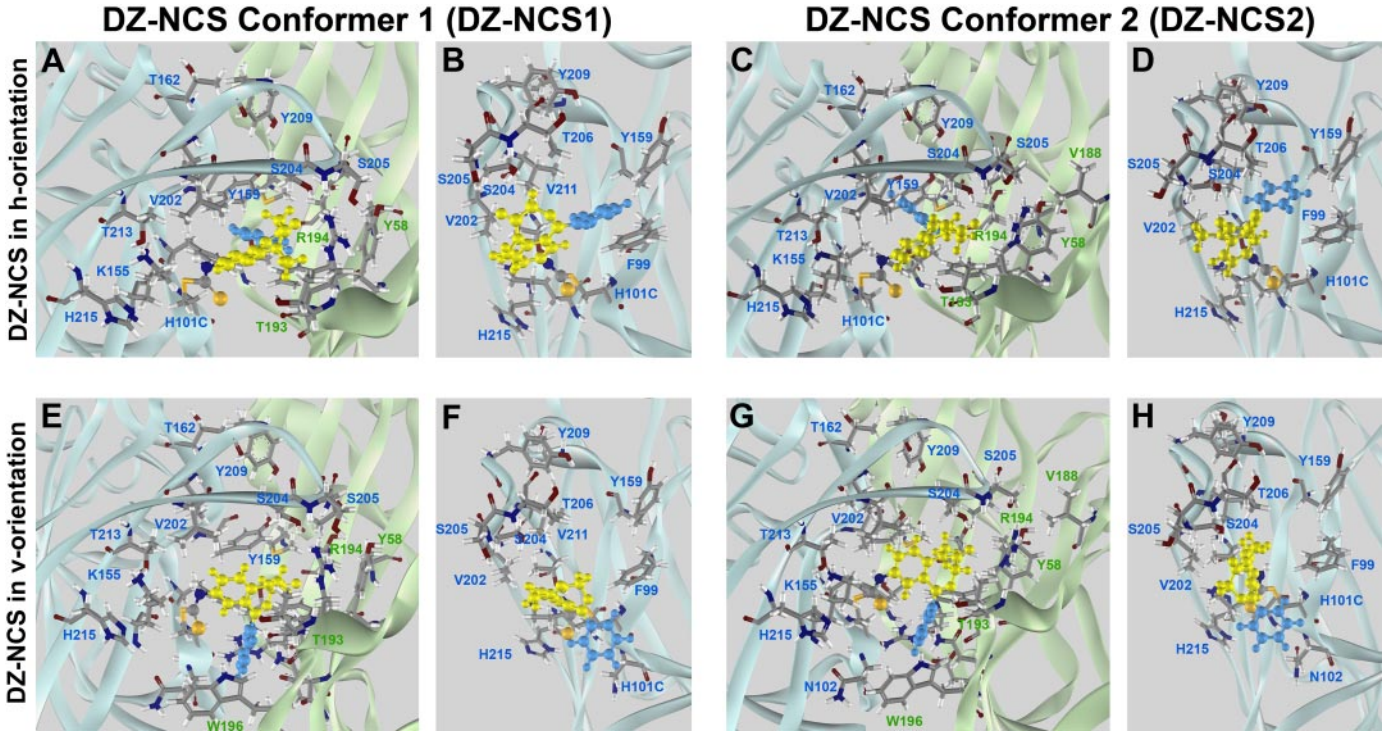

Fig. 5. Positioning of covalently bound DZ-NCS. Four energetically favorable orientations of DZ-NCS resulted from a search for lowest energy conformations via systematic rotation of the -CS-NH- bond. DZ-NCS's seven-member benzodiazepine ring is yellow and C5-phenyl is painted blue. For each conformer, low-energy binding orientations include a horizontal orientation in which the C5-phenyl group of the ligand is approximately parallel to the plasma membrane (DZ-NCS1h, A and B; DZ-NCS2h, C and D) and a vertical orientation in which the C5-phenyl extends toward the plasma membrane (DZ-NCS1v, E and F; DZ-NCS2v, G and H).

binding pocket, but we did not detect any unfavorable interaction between this residue and DZ or FNZ in either the h- or v-orientation (Table 1).

To test the structural model of the BZD recognition site, the impact of replacing FNZ with other BZD derivatives was examined. The 1,4-benzodiazepine used for initial isolation of GABA$_A$R [poly(Me-BZD), Fig. 2C] was attached to the agarose column via a polymethyl linker attached at the N1 position. High-affinity binding of the ligand was retained despite the presence of the linker, arguing that the linker must be able to extend out of the binding pocket with minimal perturbation of receptor structure. Docking studies suggest that the linker could exit the binding pocket from either the top or the side of the receptor (Fig. 8), but if the linker exits from the top, its length is probably insufficient to avoid steric interference between the receptor and the agarose resin bead (Fig. 8, C and D). In contrast, the length of the linker is adequate to avoid steric interference if the ligand is bound with the N1 substituent facing toward the side of the receptor, such that the linker can exit from the side of the receptor as depicted in Fig. 8, A and B. This requires the bound ligand to be in the h-orientation if it is in conformer 2 and in the v-orientation if it is in conformer 1.

To further evaluate the model and to assess whether active BZDs are bound in the h-orientation or the v-orientation, FNZ was replaced with a number of active and inactive BZD derivatives. Ro 5-4864 (Fig. 2B), which does not bind to $\alpha_1\beta_2\gamma_2$ GABA$_A$ receptors (Sigel et al., 1998), bears a para-substituent on the C5 phenyl that points directly toward α_1Tyr159 when in the h-orientation. This is likely to cause steric hindrance, which could explain its lack of activity; this steric clash is not present in the v-orientation. Ro 5-4654, which lacks the C5 phenyl group, is inactive (Sigel et al., 1998), arguing that interactions with this group are required for high-affinity binding of classic 1,4-benzodiazepines.

The orientation of benzodiazepines in the binding pocket was further evaluated by replacing FNZ with the active (Fig. 2D) and inactive (Fig. 2E) BZD derivatives previously studied experimentally by Zhang et al. (1994) (analogs 1–3) and by Klopman and Contreras (1985) (analog 4). Interaction energies for these analogs in each orientation were calculated (Table 2). Analogs 1 and 2, which are active in displacing [^{3}H]FNZ binding from rat brain membranes (Zhang et al., 1994), were well accommodated in the h-orientation in either conformer 1 (Fig. 9A) or conformer 2 (Fig. 9B). In contrast, there was steric hindrance for both conformers in the v-orientation (Fig. 9, C and D). Analog 3, which has little or no affinity for the BZD recognition site (Zhang et al., 1994), yielded unfavorable interaction energies in all orientations because of steric clashes with the residues and backbone of the α_1 subunit, as did analog 4, which has been reported to have very low anticonvulsant potency in vivo (Klopman and Contreras, 1985) (Fig. 10).

To evaluate whether the model reproduces the stereospecificity of BZD binding, two optically active FNZ derivatives were docked into the binding pocket. The dextrorotary Ro 11-6896, with the C3-methyl pointing up, exhibits more than 100-fold greater affinity in binding studies than its levorotatory enantiomer Ro 11-6893 (Fig. 2), which has the methyl group pointing down (Niehoff et al., 1982). In the h-orienta-

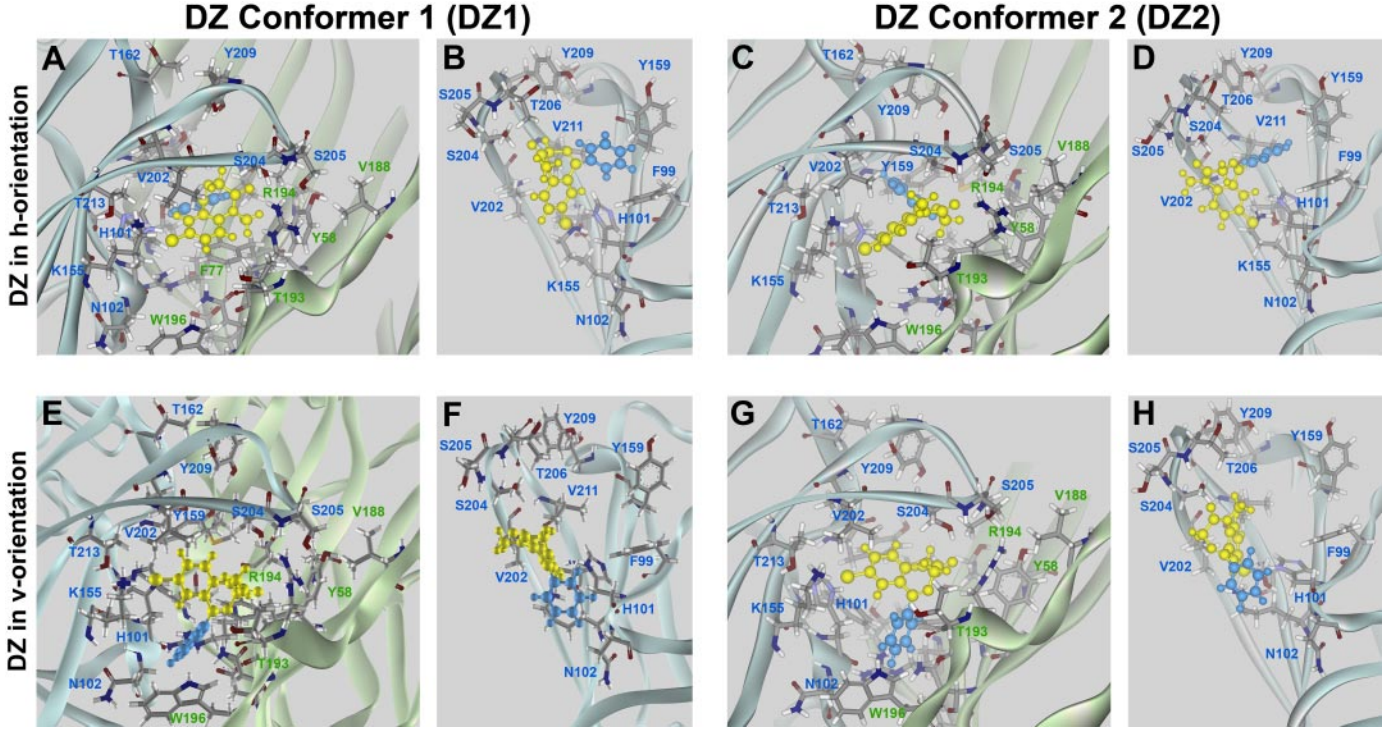

Fig. 6. Orientations of DZ were modeled after orientations of the DZ-NCS. The methyl substituent at the N1 atom of DZ is much smaller in size than the polymethyl linker used for affinity purification (Fig. 9) and is not able to restrict the ability of the benzodiazepine ring to undergo inversions, making it more difficult to deduce which of the two conformers is likely to be prevalent in the binding pocket. DZ's seven-member benzodiazepine ring is yellow, and the C5-phenyl is blue. A and B, DZ1h; C and D, DZ2h; E and F, DZ1v; G and H, DZ2v orientation. In all of these models, the C7-chloro group is directed toward the α_1His101 and α_1Lys155 residues, and the C2 carbonyl group is located in close proximity to α_1Ser204, α_1Ser205, γ_2Thr193, and γ_2Arg194, where it is able to make hydrogen bonds. Pairs of images depict the BZD binding pocket viewed from outside of the receptor (A, C, E, and G) and from within the binding pocket looking toward the α subunit (B, D, F, and H).

tion, interaction energies for these two compounds reproduced the observed stereospecificity of binding, with both conformers of Ro 11-6896 exhibiting more favorable binding energies than Ro 11-6893. For the v-orientation, results were mixed, with Ro 11-6896 being favored over Ro 11-6893 in conformer 1 but Ro 11-6893 being favored in conformer 2. The h-orientation thus best reproduces the observed stereospecific binding of these ligands (Table 3).

Automated Docking of DZ and FNZ. To assess the validity of results obtained using manual docking, automated docking was carried out using the CDocker algorithm (Wu et al., 2003), and the 20 most energetically favorable conformers were selected for further analysis. This algorithm yielded a number of models resembling the v- and h-orientations obtained by manual docking, as well as orientations that were distinct. This result can be explained by the way the docking algorithm operates: random conformations are generated and seeded within the binding pocket, and subsequent molecular dynamics and energy minimization finds a local energy minima without regard for known structure-function data. Overall, interaction energies from automated docking (Table 3) were somewhat less favorable than for manual docking, most likely because the random starting position of the ligand resulted in a less efficient optimization than in the manual search, in which the starting position for optimization was based on information derived from DZ-NCS labeling.

Automated docking yielded 3 orientations for DZ, designated DZ dock1–3, each constituting approximately one third of the total pool (Supplemental Fig. 2; interaction energies in Table 3). Two of these orientations superimpose well with manual docking orientations: DZ dock1 with DZ2h (with RMSD of 1.8 Å) and DZ dock2 with DZ2v (RMSD of 1.36 Å); DZ dock3, although favorable in energetic terms, was different from the orientations obtained by manual docking. In this orientation, the C5-phenyl group points outside the binding pocket; however, it is known that the presence of a chlorine atom at the para-position of this group (Ro 5-4864) eliminates activity. This is most likely due to steric hindrance, because chlorine in the ortho-position is tolerated (Sigel et al., 1998), indicating that the phenyl group probably does not point out of the pocket.

For FNZ, automated docking resulted in five orientations, FNZ dock1–5, respectively constituting 30, 20, 25, 5, and 20% of the total model pool. FNZ dock1 and dock2 are very similar to FNZ2v and can be superimposed with RMSDs of 0.81 and 3.04 Å (Supplemental Fig. 3, A and B), whereas FNZ dock4 and dock5 closely resemble the orientation of FNZ2h (RMSDs of 1.06 and 1.46Å, respectively) (Supplemental Fig. 3, G–J). FNZ dock3 (Supplemental Fig. 3 E and F) somewhat resembles FNZ2h but differs from it by a larger RMSD of 4.2 Å that is caused by "sinking" of the nitro-phenyl part of DZ in the intersubunit interface.

Discussion

Modeling the molecular interactions of ligands with receptors provides a means of refining structure-activity relationships to aid drug discovery. Crystallization of glutamate receptor ligand-binding domains has helped to visualize

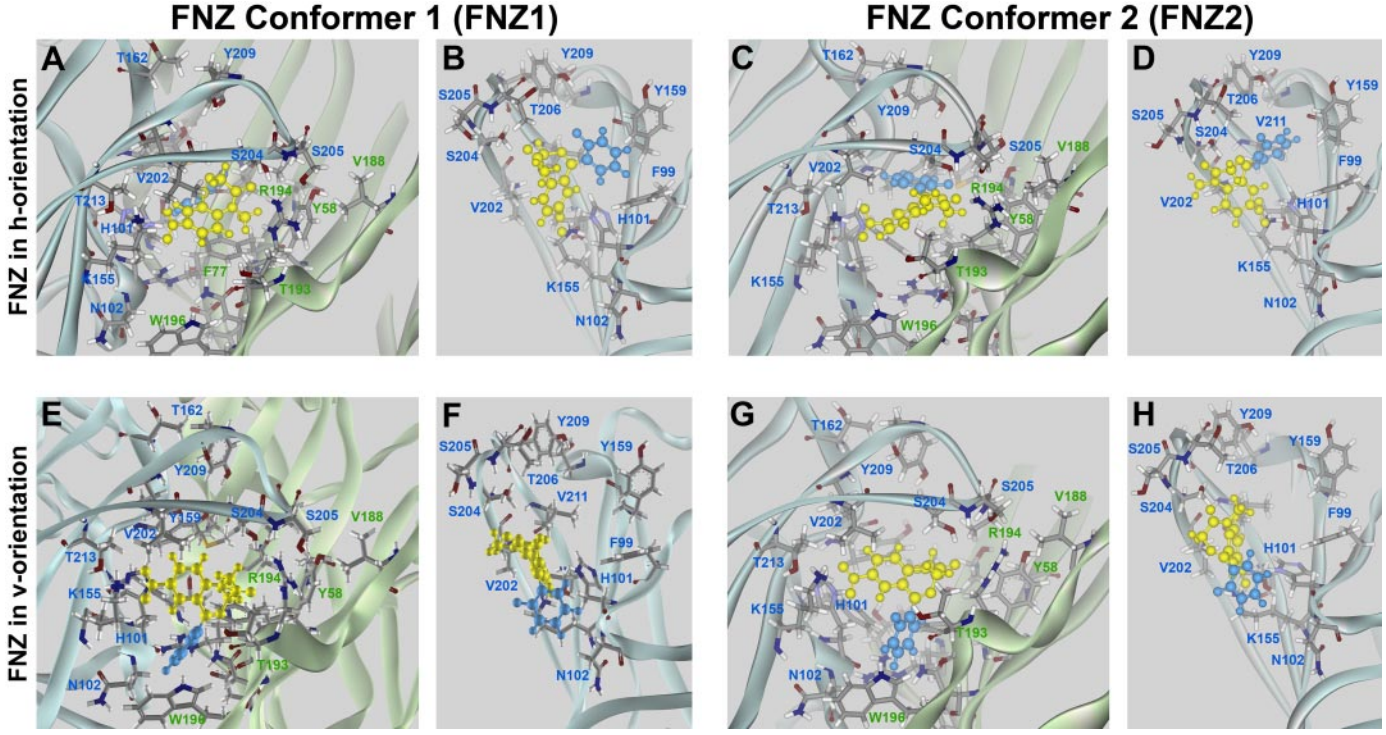

Fig. 7. Orientations of FNZ in the binding pocket were modeled after orientations of DZ-NCS. FNZ shows potency and efficacy in binding and electrophysiological assays very similar to DZ, but it differs in that it contains a nitro group, which is a strong hydrogen bond acceptor; additionally, it has a fluoro group in the ortho-position of the C5 phenyl. FNZ's seven-member benzodiazepine ring is yellow, and the C5-phenyl is blue. Binding models were generated corresponding to the h-orientation (A and B, FNZ1h; C and D, FNZ2h), and v-orientation (E and F, FNZ1v; G and H, FNZ2v). All of these models share two common features: the C7-nitro group is directed toward the α_1His101 and α_1Lys155 residues, and the C2 carbonyl group is located in close proximity to α_1Ser204, γ_2Thr193, and γ_2Arg194, where it is able to make hydrogen bonds. Pairs of images depict the BZD binding pocket viewed from outside of the receptor (A, C, E, and G) and from within the binding pocket looking toward the α subunit (B, D, F, and H).

binding pockets for agonists and allosteric modulators (Jin et al., 2005). Currently, the only structural data available for $GABA_A$Rs are enhanced electron-microscopy images of nicotinic acetylcholine receptors and X-ray structures of acetylcholine binding proteins from *Aplysia californica* (Ulens et al., 2006) and *Lymnea stagnalis* (Brejc et al., 2001; Celie et al., 2004), which share ~18% sequence identity with the $GABA_A$R extracellular domain.

The 1,4-benzodiazepine FNZ photoaffinity labels residue α_1His101 (McKernan et al., 1995; Duncalfe et al., 1996; Smith and Olsen, 2000), indicating that the FNZ nitro-group is located near this residue, but the lack of detailed information about the structure of the reaction product and the functional consequences of modification precludes precise positioning of FNZ in the binding pocket. Photoaffinity binding of FNZ blocks potentiation by chlordiazepoxide, but because only ~25% of receptors are irreversibly bound, it was not possible to determine whether FNZ photoaffinity binding results in persistent potentiation (Gibbs et al., 1985).

Exposure of α_1H101C receptors to DZ-NCS results in irreversible reduction of [^{3}H]Ro 15-1788 binding, indicating covalent binding of DZ-NCS within the binding pocket (Berezhnoy et al., 2004). A caveat is that affinity-labeling could "capture" a minor orientation that does not contribute appreciably to the action of reversibly bound BZDs. DZ-NCS also modifies α_1N102C and γ_2A79C, albeit with lower efficiency (Tan et al., 2007a), and an NCS analog of Ro 15-4513, which lacks the pendant phenyl and may have greater freedom to orient in the binding pocket, reacts with α_1 residues 101, 157, 202, and 211. Confidence that DZ-NCS covalently linked to α1 residue 101 occupies the binding pocket similarly to reversibly bound DZ is increased because α_1His101 is a known contact residue that is critical for pharmacological activity of BZDs (McKernan et al., 1995; Davies et al., 1996; Duncalfe et al., 1996; Smith and Olsen, 2000) and because covalent linkage of DZ-NCS results in irreversible potentiation comparable with that produced by DZ (Berezhnoy et al., 2004). We therefore used the position of DZ-NCS within the binding site as a basis for modeling how BZDs occupy the binding pocket.

TABLE 1

Docking energies of DZ (DZ1h, DZ1v, DZ2h, and DZ2v) and FNZ (FNZ1h, FNZ1v, FNZ2h, FNZ2v) in α_1H101R and γ_2F77Y mutant receptors

Potential energies were calculated using the Calculate Interaction Energy protocol as described under *Materials and Methods*.

Orientation	Energy		
	α_1/γ_2	α_1H101R/γ_2	α_1/γ_2F77Y
	kcal/mol		
DZ1h	−110	730	−108
DZ1v	−96	−4	−4
DZ2h	−78	290	−95
DZ2v	−77	−40	−26
FNZ1h	−330	616	−330
FNZ1v	−310	−63	−250
FNZ2h	−270	120	−310
FNZ2v	−290	−94	−280

The structure of AChBP complexed with nicotine (Celie et al., 2004), which probably reflects a high-affinity configuration of the binding pocket similar to that associated with the open or desensitized receptor (Brejc et al., 2001; Unwin et al., 2002; Celie et al., 2004), was chosen as a basis for homology modeling of the $GABA_A$R based on the hypothesis that conformational changes associated with binding of allosteric modulators to the BZD recognition site resemble those that accompany binding of nicotine to AChBP. The structural similarity of the BZD recognition site to the GABA binding site suggests that positive modulation by BZDs probably involves conformational changes similar to the activation by GABA, resulting in downstream conformational changes that stabilize the active state(s) of the receptor (Downing et al., 2005). The hypothesis that BZDs interact with their recognition site in an agonist-like manner is supported by the observation that DZ, FNZ, and zolpidem directly activate $GABA_A$ receptors containing the α_1L263S (Downing et al., 2005; Rüsch and Forman, 2005) or γ_2L245S mutations (Bianchi and Macdonald, 2001) in the absence of GABA.

The plausibility of this model is supported by the observation that, with one exception, all glycosylation sites and all residues implicated in GABA and BZD binding are exposed to water. Only one residue reported as important for FNZ binding, γ_2Met57, is buried; however, the neighboring residue, γ_2Tyr58, which also has been implicated in maintaining high-affinity binding of FNZ, is exposed, suggesting that effects of mutating γ_2Met57 may be allosteric (Kucken et al., 2000).

Modeling of the binding of DZ and FNZ yielded results similar to DZ-NCS, in which each conformer could be bound in either the h- or v-orientation. Introduction of the α_1H101R mutation, which results in 500- to 800-fold reduction in affinity of classic benzodiazepines (Wieland et al., 1992; Wieland and Lüddens, 1994; Benson et al., 1998; Dunn et al., 1999), resulted in steric clashes of arginine residues with both conformers of DZ and FNZ in the h-orientation. In contrast, this mutation was accommodated by both DZ and FNZ in the v-orientation. The h-orientation is thus more consistent with the large impact of this mutation on DZ and FNZ binding affinity.

In summary, the impact of the α1H101R mutation, the lack of activity of Ro 5-4864, the activity of analogs 1 and 2, and the higher affinity of Ro 11-6896 compared with Ro 11-6893 are consistent with the h-orientation but not the v-orienta-

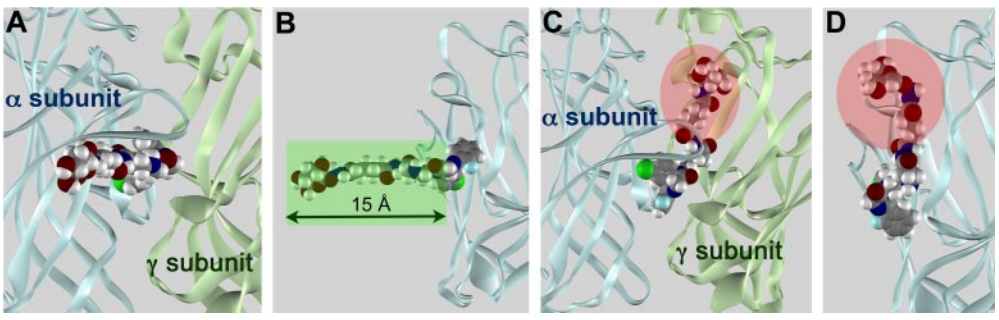

Fig. 8. Positioning of BZD ligand with polymethyl linker in binding pocket. A tethered BZD ligand was used in the affinity column for initial isolation of the $GABA_A$-R by Sigel et al. (1983). Geometry and size of this ligand suggests that the polymethyl linker can exit the binding pocket either from the side of the binding pocket (A and B) or from the top (C and D). The latter is less likely, because the length of the linker (highlighted in red in C and D) attached to the affinity column would not be expected to permit the ligand to reach the binding pocket.

tion of 1,4-BZDs in the binding pocket. In addition, the model is consistent with the success of a tethered affinity ligand in the initial purification of the $GABA_A$ receptor, and the lack of activity of analogs 3 and 4.

Although the model suggests that DZ and FNZ should be able to bind in either the h-orientation or the v-orientation, evidence suggests that this does not occur. The profound impact of the α1H101R mutation on binding of DZ and FNZ is inconsistent with the modest effect of this mutation on the binding energies of these two ligands in the v-orientation, arguing that little if any binding occurs in this orientation. It is unclear why the v-orientation is not realized in practice. In addition to the uncertainties inherent in a homology model that is derived from the crystal structure of a different protein binding a different ligand, a crystal structure represents a static "snapshot" of binding, and does not reproduce the conformational changes that probably occur in the initial interaction between ligand and receptor.

In addition, the model was unable to explain the effects of the γ_2F77Y mutation, which reduces DZ and FNZ binding affinities by 230- and 170-fold, respectively, but did not result in steric clashes between DZ or FNZ and γ_2F77Y for any of conformers/orientations tested. This may indicate the existence of an additional favorable orientation in which the BZ directly contacts this residue, as proposed by Sancar et al. (2007); however, the introduction of nonaromatic γ_2F77L,

TABLE 2

Interaction energies of analogs 1 to 4

Interaction energies (potential, van der Waals, and electrostatic energies) of receptor and affinity probes were calculated for each basic orientation as described under *Materials and Methods* using the Calculate Interaction Energy protocol.

Conformers and Analog Nos.	Energy
	kcal/mol
Conformer 1 h	
1 (active)	−73
2 (active)	−61
3 (inactive)	$>7 \times 10^7$
4 (inactive)	$>1 \times 10^8$
Conformer 2 h	
1 (active)	−37
2 (active)	−49
3 (inactive)	560,000
4 (inactive)	$>1 \times 10^{12}$
Conformer 1v	
1 (active)	580
2 (active)	320
3 (inactive)	3600
4 (inactive)	1700
Conformer 2v	
1 (active)	$>1 \times 10^9$
2 (active)	290
3 (inactive)	$>2 \times 10^9$
4 (inactive)	$>1 \times 10^7$

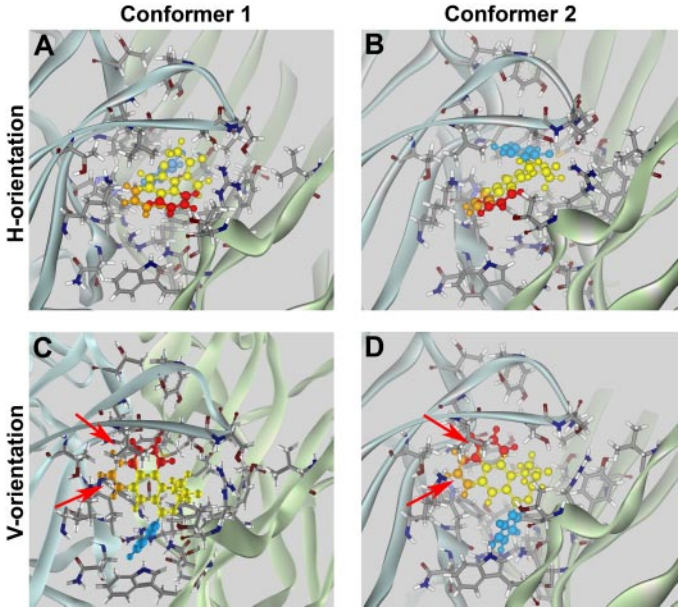

Fig. 9. Docking of active BZD analogs. Models of FNZ binding obtained in manual docking runs were tested using analogs 1 (red-yellow-blue) and 2 (orange-yellow-blue) (Fig. 2), which bind with moderate affinities (260 and 55 nM, respectively; Zhang et al., 1994). Each analog was docked as conformer 1 (A and C) or conformer 2 (B and D) in the h-orientation (A and B) or v-orientation (C and D). Both analogs interacted favorably in conformer 1 or 2 in the h-orientation (A and B). In the v-orientation (C and D), both analogs exhibited steric interference with residues α_1His101 and α_1Lys155 (red arrows), resulting in highly unfavorable interaction energies for both conformers (Table 1).

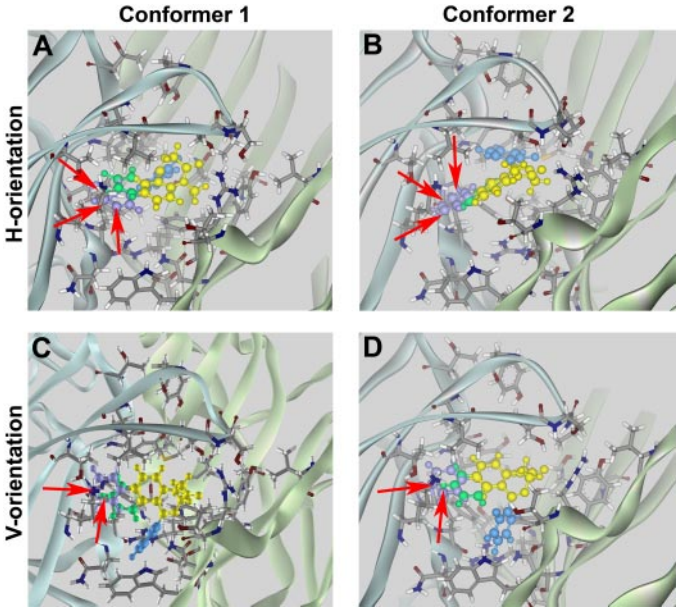

Fig. 10. Docking of inactive BZD analogs. Models of FNZ binding obtained in manual docking runs were tested using analogs 3 and 4 depicted in Fig. 2. Analogs 3 (green-yellow-blue) (Zhang et al., 1994) and 4 (violet-yellow-blue) (Klopman and Contreras, 1985) are inactive. Both analogs exhibited steric clashes (red arrows) with residues α_1His101 and α_1Lys155 when docked as conformer 1 (A and C) or conformer 2 (B and D) in either the h-orientation (A and B) or the v-orientation (C and D).

TABLE 3

Docking energies of Ro 11-6896 abbreviated Me(+) in different orientations [Me1(+) h, Me1(+) v, Me2(+) h, and Me2(+) v] and Ro 11-6893 abbreviated Me(−) in different orientations [Me1(−) h, Me1(−) v, Me2(−) h, and Me2(−) v]

Potential energies were calculated using the Calculate Interaction Energy protocol as described under *Materials and Methods*.

Orientation	Energy
	kcal/mol
Me1(+) h	−78
Me1(−) h	34
Me2(+) h	−110
Me2(−) h	−54
Me1(+) v	−91
Me1(−) v	−29
Me2(+) v	150
Me2(−) v	−47

γ_2F77I, or bulky γ_2F77W residues at this position produces only modest effects on DZ and FNZ affinity (Buhr et al., 1997), whereas introduction of γ_2F77C completely abolishes FNZ binding (Teissére and Czajkowski, 2001). The lack of correlation with residue volume suggests that the effect of this mutation may relate to conformational changes associated with receptor activation, rather than binding, which may not be reflected by our model.

In a recent study, Sancar et al. (2007) reported automated docking of FNZ and zolpidem, which resulted in a FNZ position that differs significantly from our results. In this model, the N1-methyl substituent is directed toward the membrane and is buried in the binding site, the carboxyl group is in close proximity to γ_2Arg144 and α_1Thr206, and a fluorine atom is located next to α_1Tyr209, with γ_2Thr193 and γ_2Arg194 located close to C5-phenyl moiety. Sancar et al. (2007) reported that the γ_2R194D mutation produced no change in [^{3}H]FNZ binding affinity, whereas Padgett and Lummis (2008) found that γ_2R194N and γ_2R194K mutations reduced maximum DZ potentiation of $\alpha_1\beta_2\gamma_2$ receptors by 2.5- and 4-fold, respectively, whereas mutation of the neighboring residue γ_2Ser195 to threonine reduced DZ potentiation by 5-fold. These results, which indicate that mutations of loop F influence BZD efficacy rather than potency, suggest that conformational changes within loop F are coupled to receptor activation.

By inspection of the proximity of residues facing the ligand in the present model (Supplementary Table 2), we were not able to identify specific bonds or interactions that were dominant. Rather, the key observation of this study is one of ligand orientation. However, some predictions from this model may be informative. First, loop F is located near loop C such that γ_2Arg194 is near α_1Ser204/α_1Ser205, whereas γ_2Thr193 is close to γ_2Trp196/γ_2Arg197. This arrangement would permit the formation of hydrogen bonds within these residue triads, possibly coordinating with the carboxyl group of DZ or FNZ. This orientation is supported by the recent findings of Tan et al. (2007b), who discovered that a DZ-NCS analog with a reactive group in the 3-position of the benzodiazepine ring covalently labels α_1Ser205 and α_1Thr206. It is possible then that this may reflect an activated configuration of the binding pocket. Second, hydrogen bonds may also form between α_1Lys155 and the FNZ nitro group oxygen atoms. Finally, π–π interactions could occur between the α_1Tyr159 and α_1Tyr209 and the pendant phenyl moiety.

The present study focuses on the orientation of classic BZDs in the binding pocket, and it is unclear whether non-BZD ligands orient similarly; however, mutagenesis and docking studies of the non-BZD ligands zolpidem and eszopiclone indicate that interactions with α_1His101, α_1Ser204, and γ_2Arg194 contribute to orienting these ligands in the binding pocket (Hanson et al., 2008).

In this study, we attempted to integrate the available structure-activity data on the interaction of the most studied class of BZD binding site ligands with the structure-function data for the most studied $GABA_A$R isoform. Docking to a molecular model for the BZD recognition site indicates that the key structural elements of classic 1,4-benzodiazepines, the 1,4-benzodiazepine ring and the pharmacologically crucial C5-phenyl group, most likely are oriented in the binding pocket in parallel to the plasma membrane and perpendicular to the Cl^- channel. Application of this computational modeling strategy, which integrates site-directed affinity labeling with structure-activity knowledge to create a molecular model of the docking of active ligands in the binding pocket, may provide a basis for the design of novel $GABA_A$R modulators with enhanced therapeutic potential.

References

Barnard EA, Skolnick P, Olsen RW, Mohler H, Sieghart W, Biggio G, Braestrup C, Bateson AN, and Langer SZ (1998) International Union of Pharmacology. XV. Subtypes of gamma-aminobutyric acidA receptors: classification on the basis of subunit structure and receptor function. *Pharmacol Rev* **50:**291–313.

Benson JA, Löw K, Keist R, Mohler H, and Rudolph U (1998) Pharmacology of recombinant γ-aminobutyric acid A receptors rendered diazepam-insensitive by point-mutated receptors. *FEBS Lett* **431:**400–404.

Berezhnoy D, Gravielle MC, and Farb DH (2007) Pharmacology of the $GABA_A$ receptor, in *Handbook of Contemporary Neuropharmacology* (Sibley D, Hanin I, Kuhar M, and Skolnick P eds) vol 1, pp 465–568, John Wiley & Sons/Wiley-Interscience, Hoboken, NJ.

Berezhnoy D, Baur R, Gonthier A, Foucaud B, Goeldner M, and Sigel E (2005) Conformational changes at benzodiazepine binding sites of $GABA_A$ receptors detected with a novel technique. *J Neurochem* **92:**859–866.

Berezhnoy D, Nyfeler Y, Gonthier A, Schwob H, Goeldner M, and Sigel E (2004) On the benzodiazepine binding pocket in $GABA_A$ receptors. *J Biol Chem* **279:**3160–3168.

Bianchi MT and Macdonald RL (2001) Agonist trapping by $GABA_A$ receptor channels. *J Neurosci* **21:**9083–9091.

Blount JF, Fryer RI, Gilman NW, and Todaro LJ (1983) Quinazolines and 1,4-benzodiazepines. 92. Conformational recognition of the receptor by 1,4-benzodiazepines. *Mol Pharmacol* **24:**425–428.

Bonnert TP, McKernan RM, Farrar S, le Bourdellès B, Heavens RP, Smith DW, Hewson L, Rigby MR, Sirinathsinghji DJ, Brown N, et al. (1999) Theta, a novel γ-aminobutyric acid type A receptor subunit. *Proc Natl Acad Sci U S A* **96:**9891–9896.

Borea PA, Gilli G, Bertolasi V, and Ferretti V (1987) Stereochemical features controlling binding and intrinsic activity properties of benzodiazepine-receptor ligands. *Mol Pharmacol* **31:**334–344.

Brejc K, van Dijk WJ, Klaassen RV, Schuurmans M, van Der Oost J, Smit AB, and Sixma TK (2001) Crystal structure of an ACh-binding protein reveals the ligand-binding domain of nicotinic receptors. *Nature* **411:**269–276.

Buhr A, Baur R, and Sigel E (1997) Subtle changes in residue 77 of the γ subunit of $\alpha_1\beta_2\gamma_2$ $GABA_A$ receptors drastically alter the affinity for ligands of the benzodiazepine binding site. *J Biol Chem* **272:**11799–11804.

Camerman A and Camerman N (1972) Stereochemical basis of anticonvulsant drug action. II. Molecular structure of diazepam. *J Am Chem Soc* **94:**268–272.

Celie PH, van Rossum-Fikkert SE, van Dijk WJ, Brejc K, Smit AB, and Sixma TK (2004) Nicotine and carbamylcholine binding to nicotinic acetylcholine receptors as studied in AChBP crystal structures. *Neuron* **41:**907–914.

Chan CY and Farb DH (1985) Modulation of neurotransmitter action: control of the gamma-aminobutyric acid response through the benzodiazepine receptor. *J Neurosci* **5:**2365–2373.

Choh DW, Farb DH, and Fischbach GD (1977) Chlordiazepoxide selectively augments GABA action in spinal cord cell cultures. *Nature* **269:**342–344.

Davies M, Martin IL, Bateson AN, Hadingham KL, Whiting PJ, and Dunn SM (1996) Identification of domains in human recombinant $GABA_A$ receptors that are photoaffinity labelled by [^{3}H]flunitrazepam and [^{3}H]Ro 15-4513. *Neuropharmacology* **35:**1199–1208.

De Blas AL, Sangameswaran L, Haney SA, Park D, Abraham CJ Jr, and Rayner CA (1985) Monoclonal antibodies to benzodiazepines. *J Neurochem* **45:**1748–1753.

Downing SS, Lee YT, Farb DH, and Gibbs TT (2005) Benzodiazepine modulation of partial agonist efficacy and spontaneously active $GABA_A$ receptors supports an allosteric model of modulation. *Br J Pharmacol* **145:**894–906.

Duncalfe LL, Carpenter MR, Smillie LB, Martin IL, and Dunn SM (1996) The major site of photoaffinity labeling of the γ-aminobutyric acid type A receptor by [^{3}H]flunitrazepam is histidine 102 of the α subunit. *J Biol Chem* **271:**9209–9214.

Dunn SM, Davies M, Muntoni AL, and Lambert JJ (1999) Mutagenesis of the rat α1 subunit of the γ-aminobutyric $acid_A$ receptor reveals the importance of residue 101 in determining the allosteric effects of benzodiazepine site ligands. *Mol Pharmacol* **56:**768–774.

Gibbs TT, Chan CY, Czajkowski CM, and Farb DH (1985) Benzodiazepine receptor photoaffinity labeling: correlation of function with binding. *Eur J Pharmacol* **110:**171–180.

Hanson SM, Morlock EV, Satyshur KA, and Czajkowski C (2008) Structural requirements for eszopiclone and zolpidem binding to the gamma-aminobutyric acid type-A (GABAA) receptor are different. *J Med Chem* **51:**7243–7252.

He X, Huang Q, Ma C, Yu S, McKernan R, and Cook JM (2000) Pharmacophore/receptor models for $GABA_A$/BzR alpha2beta3gamma2, alpha3beta3gamma2 and alpha4beta3gamma2 recombinant subtypes. Included volume analysis and comparison to alpha1beta3gamma2, alpha5beta3gamma2, and alpha6beta3gamma2 subtypes. *Drug Des Discov* **17:**131–171.

Huang Q, Cox ED, Gan T, Ma C, Bennett DW, McKernan RM, and Cook JM (1999) Studies of molecular pharmacophore/receptor models for $GABA_A$/benzodiazepine receptor subtypes: binding affinities of substituted beta-carbolines at recombinant alpha x beta 3 gamma 2 subtypes and quantitative structure-activity relationship studies via a comparative molecular field analysis. *Drug Des Discov* **16:**55–76.

Huang Q, Liu R, Zhang P, He X, McKernan R, Gan T, Bennett DW, and Cook JM (1998) Predictive models for $GABA_A$/benzodiazepine receptor subtypes: studies of quantitative structure-activity relationships for imidazobenzodiazepines at five

recombinant $GABA_A$/benzodiazepine receptor subtypes [alphaxbeta3gamma2 (x = 1–3, 5, and 6)] via comparative molecular field analysis. *J Med Chem* **41:**4130–4142.
Jin R, Clark S, Weeks AM, Dudman JT, Gouaux E, and Partin KM (2005) Mechanism of positive allosteric modulators acting on AMPA receptors. *J Neurosci* **25:**9027–9036.
Klopman G and Contreras R (1985) Use of artificial intelligence in the structure-activity correlation of anticonvulsant drugs. *Mol Pharmacol* **27:**86–93.
Kotzyba-Hibert F, Kapfer I, and Goeldner M (1995) Recent trends in photoaffinity labeling. *Angew Chem Int Ed Engl* **34:**1296–1312.
Kucken AM, Teissére JA, Seffinga-Clark J, Wagner DA, and Czajkowski C (2003) Structural requirements for imidazobenzodiazepine binding to $GABA_A$ receptors. *Mol Pharmacol* **63:**289–296.
Kucken AM, Wagner DA, Ward PR, Teissére JA, Boileau AJ, and Czajkowski C (2000) Identification of benzodiazepine binding site residues in the γ2 subunit of the γ-aminobutyric acid A receptor. *Mol Pharmacol* **57:**932–939.
Marder M, Estiú G, Blanch LB, Viola H, Wasowski C, Medina JH, and Paladini AC (2001) Molecular modeling and QSAR analysis of the interaction of flavone derivatives with the benzodiazepine binding site of the $GABA_A$ receptor complex. *Bioorg Med Chem* **9:**323–335.
McKernan RM, Wafford K, Quirk K, Hadingham KL, Harley EA, Ragan CI, and Whiting PJ (1995) The pharmacology of the benzodiazepine site of the GABA-A receptor is dependent upon the type of γ-subunit present. *J Recept Signal Transduct Res* **15:**173–183.
Niehoff DL, Mashal RD, Horst WD, O'Brien RA, Palacios JM, and Kuhar MJ (1982) Binding of a radiolabeled triazolopyridazine to a subtype of benzodiazepine receptor in the rat cerebellum. *J Pharmacol Exp Ther* **221:**670–675.
Padgett CL and Lummis SC (2008) The F-loop of the $GABA_A$ receptor γ2 subunit contributes to benzodiazepine modulation. *J Biol Chem* **283:**2702–2708.
Rüsch D and Forman SA (2005) Classic benzodiazepines modulate the open-close equilibrium in alpha1beta2gamma2L gamma-aminobutyric acid type A receptors. *Anesthesiology* **102:**783–792.
Sancar F, Ericksen SS, Kucken AM, Teissére JA, and Czajkowski C (2007) Structural determinants for high-affinity zolpidem binding to GABA-A receptors. *Mol Pharmacol* **71:**38–46.
Sawyer GW, Chiara DC, Olsen RW, and Cohen JB (2002) Identification of the bovine gamma-aminobutyric acid residues photolabeled by the imidazobenzodiazepine [^{3}H]Ro15-4513. *J Biol Chem* **277:**50036–50045.
Schove LT, Perez JJ, and Loew GH (1994) Molecular determinants of recognition and activation at the cerebellar benzodiazepine receptor site. *Bioorg Med Chem* **2:**1029–1049.
Sieghart W and Sperk G (2002) Subunit composition, distribution and function of $GABA_A$ receptor subtypes. *Curr Top Med Chem* **2:**795–816.
Sigel E and Barnard EA (1984) A γ-aminobutyric acid/benzodiapzepine receptor complex from bovine cerebral cortex: improved purification with preservation of regulatory sites and their regulations. *J Biol Chem* **259:**7129–7223.
Sigel E, Schaerer MT, Buhr A, and Baur R (1998) The benzodiazepine binding pocket of recombinant α1β2γ2 γ-aminobutyric acid A receptors: relative orientation of ligands and amino acid side chains. *Mol Pharmacol* **54:**1097–1105.
Sigel E, Stephenson FA, Mamalaki C, and Barnard EA (1983) A γ-aminobutyric acid/benzodiazepine receptor complex from bovine cerebral cortex. *J Biol Chem* **258:**6965–6971.
Smith GB and Olsen RW (1994) Identification of a [^{3}H]muscimol photoaffinity substrate in the γ-aminobutyric acid A receptor α subunit. *J Biol Chem* **269:**20380–20387.
Smith GB and Olsen RW (2000) Deduction of amino acid residues in the $GABA_A$ receptor alpha subunits photoaffinity labeled with the benzodiazepine flunitrazepam. *Neuropharmacology* **39:**55–64.
Tan KR, Baur R, Gonthier A, Goeldner M, and Sigel E (2007a) Two neighboring residues of loop A of the alpha1 subunit point towards the benzodiazepine binding site of $GABA_A$ receptors. *FEBS Lett* **581:**4718–4722.
Tan KR, Baur R, Gonthier A, Goeldner M, and Sigel E (2007b) The binding site for benzodiazepines on $GABA_A$ receptors. *Soc Neurosci Abstr* **33:**141.11.
Tan KR, Gonthier A, Baur R, Ernst M, Goeldner M, and Sigel E (2007c) Proximity-accelerated chemical coupling reaction in the benzodiazepine-binding site of γ-aminobutyric acid type A receptors: superposition of different allosteric modulators. *J Biol Chem* **282:**26316–26325.
Teissére JA and Czajkowski C (2001) β-Strand in the γ2 subunit lines the benzodiazepine binding site of the $GABA_A$ receptor: structural rearrangements detected during channel gating. *J Neurosci* **21:**4977–4986.
Thompson JD, Higgins DG, and Gibson TJ (1994) CLUSTAL W: improving the sensitivity of progressive multiple sequence alignment through sequence weighting, position-specific gap penalties and weight matrix choice. *Nucleic Acids Res* **22:**4673–4680.
Ulens C, Hogg RC, Celie PH, Bertrand D, Tsetlin V, Smit AB, and Sixma TK (2006) Structural determinants of selective α-conotoxin binding to a nicotinic acetylcholine receptor homolog AChBP. *Proc Natl Acad Sci U S A* **103:**3615–3620.
Unwin N (2003) Structure and action of the nicotinic acetylcholine receptor explored by electron microscopy. *FEBS Lett* **555:**91–95.
Unwin N, Miyazawa A, Li J, and Fujiyoshi Y (2002) Activation of the nicotinic acetylcholine receptor involves a switch in conformation of the alpha subunits. *J Mol Biol* **319:**1165–1176.
Verli H, Albuquerque MG, Bicca de Alencastro R, and Barreiro EJ (2002) Local intersection volume: a new 3D descriptor applied to develop a 3D-QSAR pharmacophore model for benzodiazepine receptor ligands. *Eur J Med Chem* **37:**219–229.
Villar HO, Uyeno ET, Toll L, Polgar W, Davies MF, and Loew GH (1989) Molecular determinants of benzodiazepine receptor affinities and anticonvulsant activities. *Mol Pharmacol* **36:**589–600.
Wieland HA, Lüddens H, and Seeburg PH (1992) A single histidine in $GABA_A$ receptors is essential for benzodiazepine agonist binding. *J Biol Chem* **267:**1426–1429.
Wieland HA and Lüddens H (1994) Four amino acid exchanges convert a diazepam-insensitive, inverse agonist-preferring $GABA_A$ receptor into a diazepam preferring $GABA_A$ receptor. *J Med Chem* **37:**4576–4580.
Wu G, Robertson DH, Brooks CL 3rd, and Vieth M (2003) Detailed analysis of grid-based molecular docking: a case study of CDOCKER—A CHARMm-based MD docking algorithm. *J Comput Chem* **24:**1549–1562.
Zhang W, Koehler KF, Harris B, Skolnick P, and Cook JM (1994) Synthesis of benzo-fused benzodiazepines employed as probes of the agonist pharmacophore of benzodiazepine receptors. *J Med Chem* **37:**745–757.
Zhang W, Koehler KF, Zhang P, and Cook JM (1995) Development of a comprehensive pharmacophore model for the benzodiazepine receptor. *Drug Des Discov* **12:**193–248.

Address correspondence to: Dr. David H. Farb, Laboratory of Molecular Neurobiology, Department of Pharmacology and Experimental Therapeutics, Boston University School of Medicine, 72 East Concord Street, L-603, Boston, MA 02118. E-mail: dfarb@bu.edu